Electronic Supplementary Material (ESI) for Journal of Materials Chemistry A.


# Supporting Information

## Stretchable and Durable Superhydrophobicity That Acts both in Air and Under Oil

A. M. Rather and U. Manna

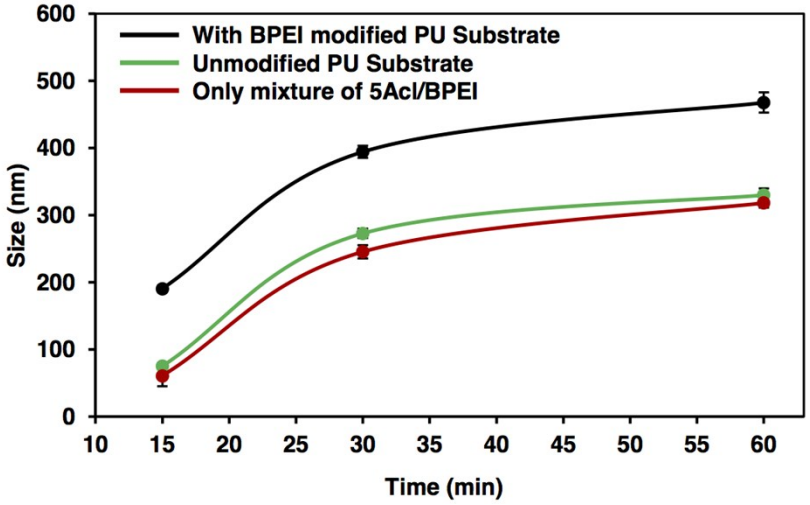


**Figure S1.** The DLS study illustrating the growth of the reactive nano-complex (RNC) in the mixture of 5-Acl/BPEI in ethanol in absence (red) and in presence of unmodified (green) and BPEI-modified (black) PU fibrous substrate with time

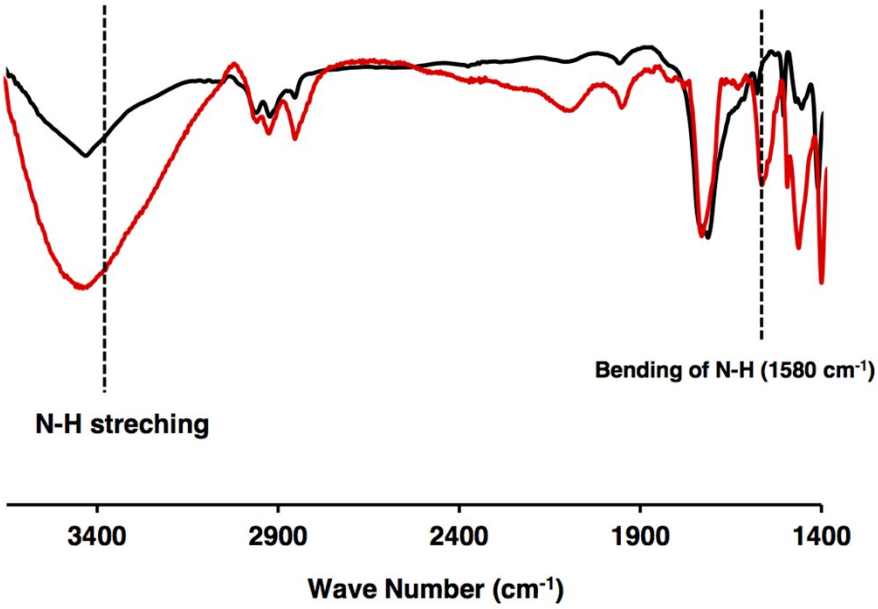


**Figure S2.** FTIR spectra of unmodified (black) and BPEI treated PU substrate (red). The peak at 3315 $cm^{-1}$ and 1580 $cm^{-1}$ are characteristic signature of N-H stretching and N-H bending respectively appeared due to successful modification of PU fibrous substrate with BPEI polymer

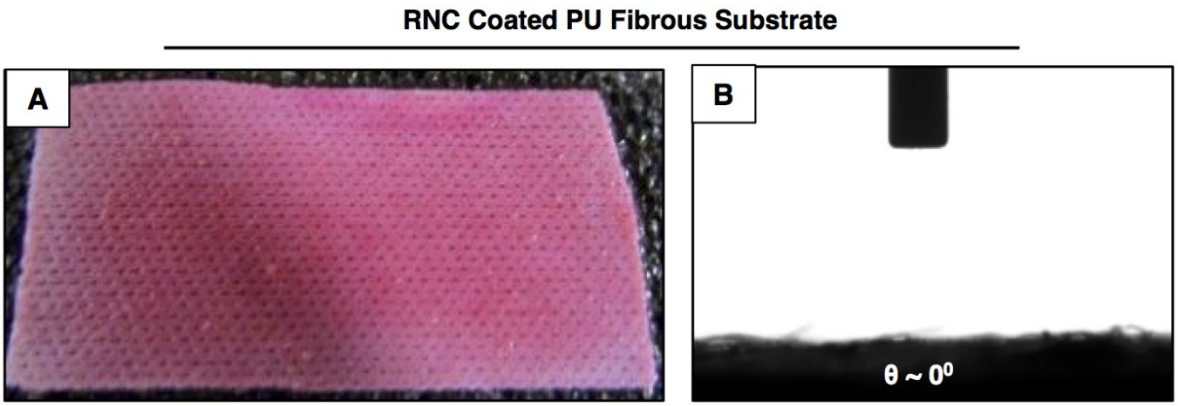


**Figure S3**. A-B) digital image (A) and contact angle image (B) of beaded water droplet on the 'reactive' nanocomplex (RNC) coated PU fibrous substrate before post chemical modification with appropriate amines.

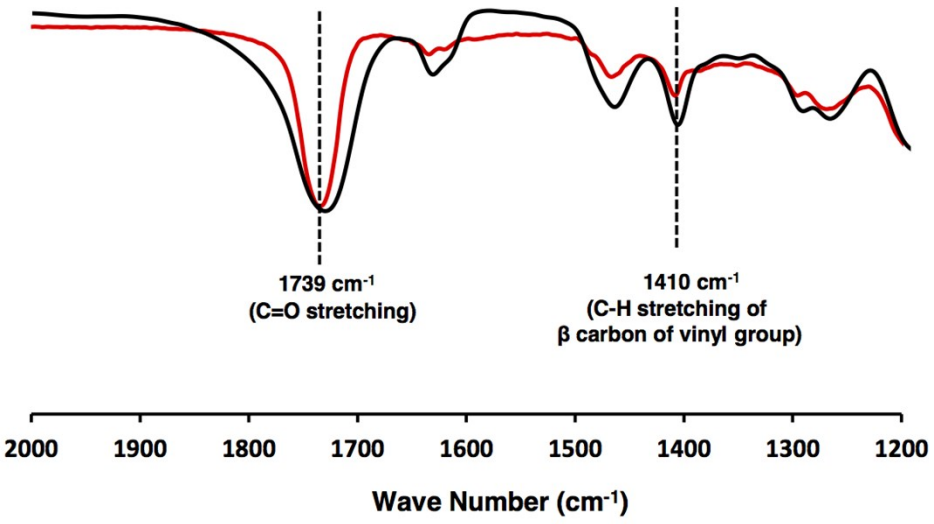


**Figure S4**. FTIR spectra of nano-complex before (black) and after (red) post-chemical treatment with octadecylamine molecules, the peaks at 1736 $cm^{-1}$ and 1410 $cm^{-1}$ denoted the carbonyl stretching and symmetric deformation of the C–H bond for the β carbon of the vinyl group respectively.

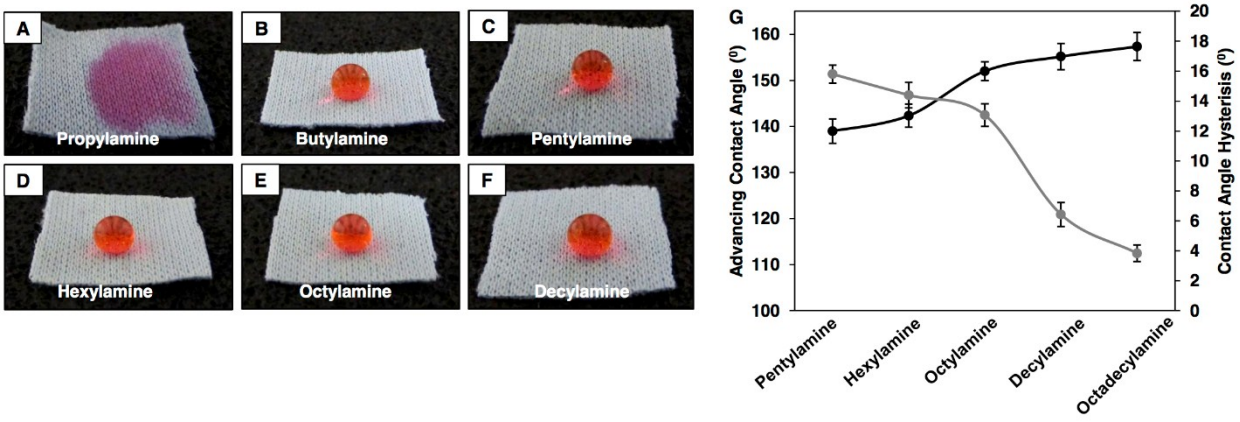


**Figure S5.** A-F) Digital images depicting the wettability of liquid water (red color aids visual inspection) on the RNC coated PU substrate after post-chemical modification with various amine containing small molecules including propylamine (A), butylamine (B), pentylamine (C), hexylamine (D), octylamine (E) and decylamine (F). G) The plot accounting the advancing contact angle (black) and contact angle hysteresis (grey) of beaded water droplets on the RNC coated PU substrate after various post-chemical functionalization

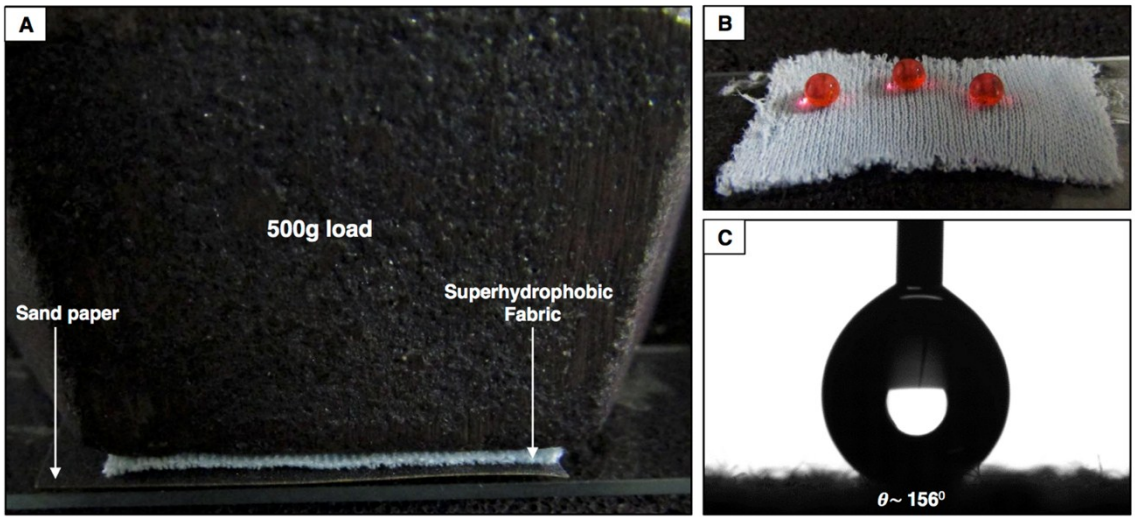


**Figure S6.** A) Experimental setup for sand paper abrasion test, where superhydrophobic PU fabric was exposed to one of the surface of the sand paper (another side is attached with microscopic glass slide through double-sided adhesive tape) and superhydrophobic PU substrate was immobilized on 500 g load with adhesive tape. Finally, the PU substrate was manually moved back and forth multiple times (five times) on the sand paper under 500 g load. B-C) Digital image (B) and water contact angle image (C) of beaded water droplet on the superhydrophobic PU substrate after sand paper abrasion

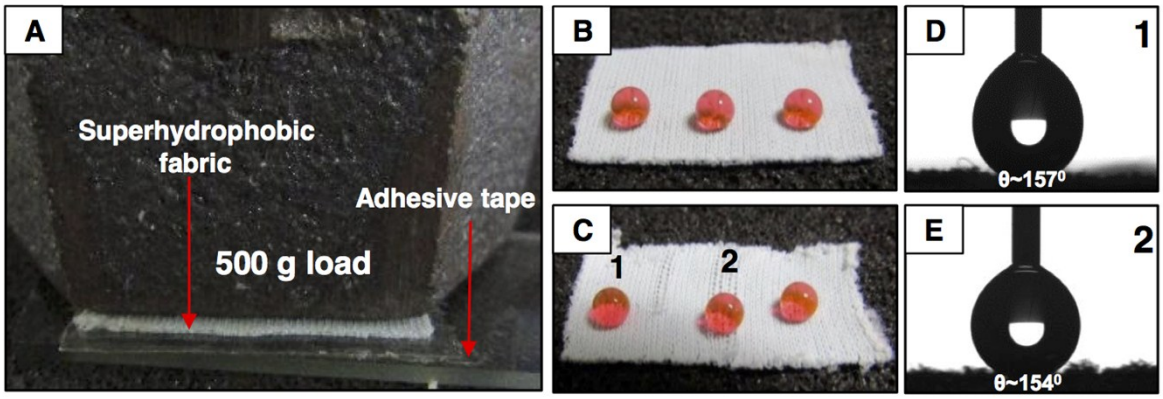


**Table 1. Advancing and Hysteresis Contact Angle Data of Various Physical Stability Tests**

| Tests | Advanced Contact Angle ($^0$) | Contact Angle Hysteresis ($^0$) |
|---|---|---|
| Adhesive Tape | 154.2±0.2 | 6.2 |
| Sand Drop | 156.3±0.5 | 4.9 |
| Creasing | 156.1±0.2 | 5.1 |
| Twisting | 155.8±0.3 | 4.8 |

**Figure S7**. A) Experimental setup for adhesive tape test, where superhydrophobic PU fabric was exposed to one of the surface of the double sided adhesive tape (another side is attached with microscopic glass slide). Then 500 gm load is applied on the material to facilitate better contact between adhesive tape and superhydrophobic PU fabric. Finally the PU fabric was manually peeled off from the double sided adhesive tape. B-E) Digital images (B-C) and contact angle images (D-E) are showing the beading of water droplet on the superhydrophobic PU substrate before (B,D) and after (C,E) adhesive tape test.

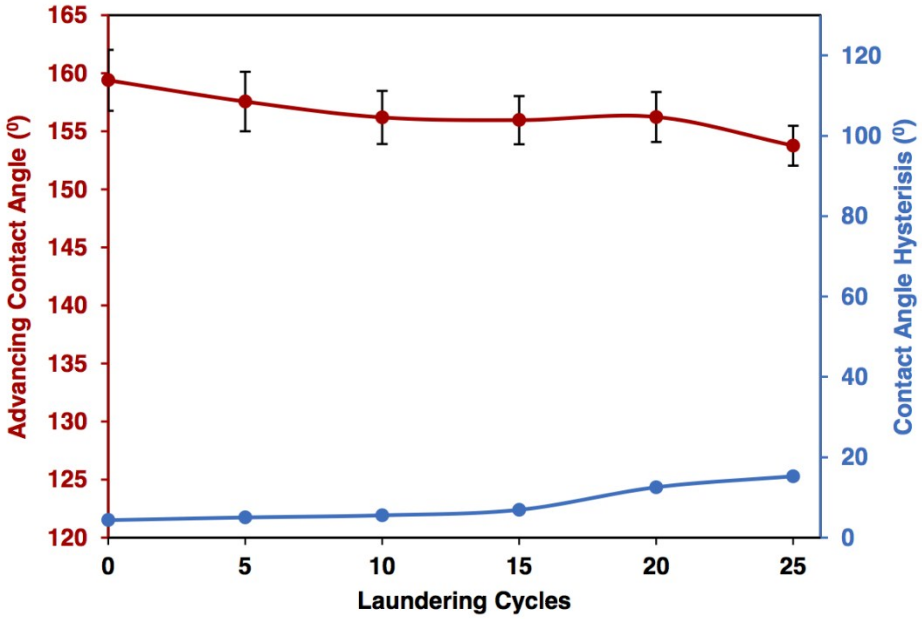


**Figure S8**. The plot accounts the effect of successive (25 times) laundering tests on the water wettability of the superhydrophobic membrane.

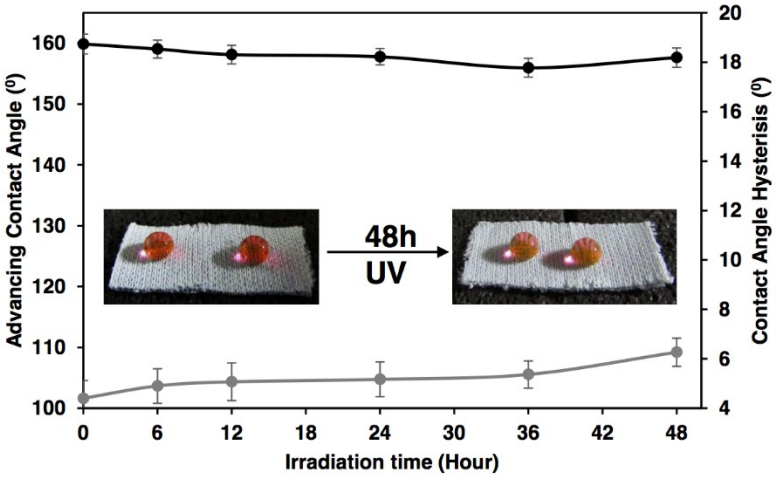


**Figure S9**. The plot illustrating the effect of prolonged (48 h) exposure of UV light (at 254 nm) on the wettability of the synthesized material.

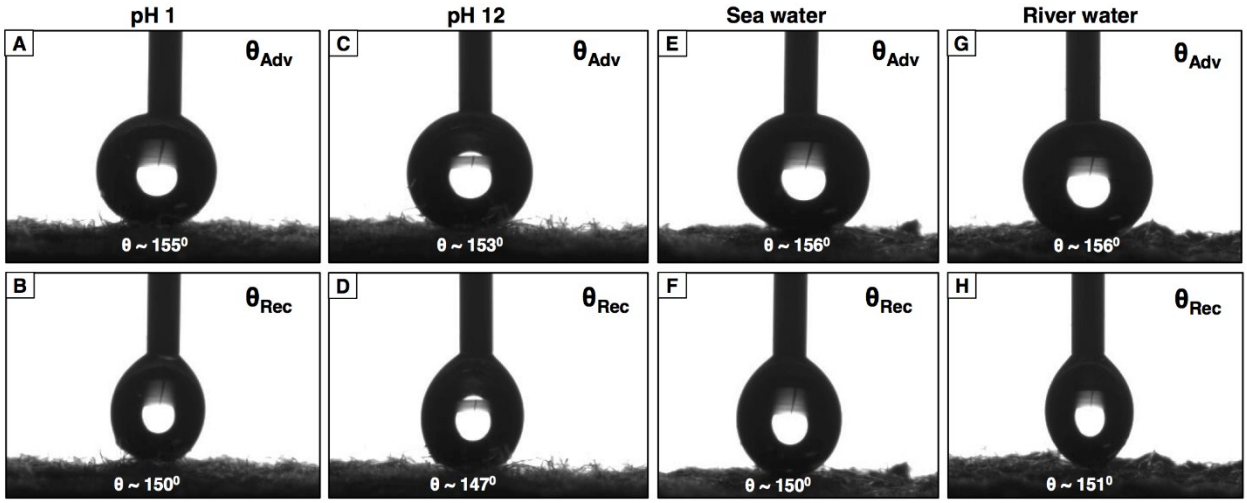


**Figure S10**. A-H) Advancing (A, C, E, G) and receding (B, D, F, H) water contact angle images of the beaded water droplets on the superhydrophobic membrane after continuous exposure to complex aqueous phases (including pH 1 (A-B), pH 12 (C-D), sea water (E-F), River water (G-H)) for 48 h.

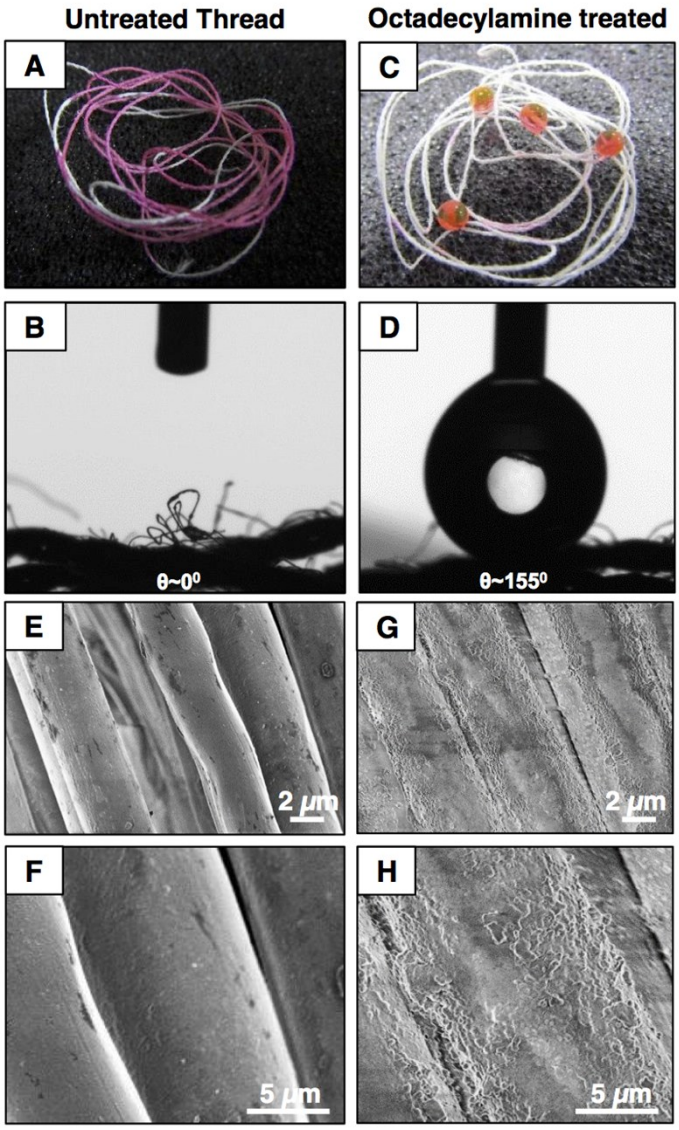


**Figure S11**. A-D) Digital images(A, C) and contact angle images (B, D) of RNC coated cotton thread with beaded water droplets before (A, B) and after post modification with octadecylamine (C, D). E-H) FESEM images of uncoated cotton thread (E, F) and after reactive nano-complex immobilization (G, H) at low (E, G) and high magnifications (F, H).

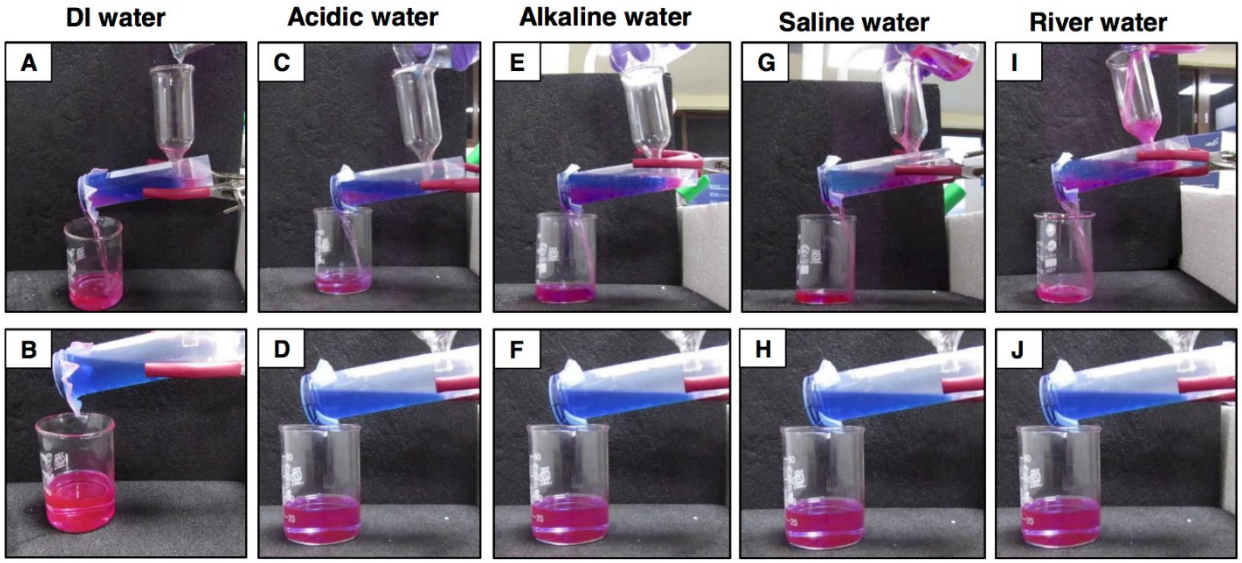


**Figure S12**. (A-J) Digital images accounting separation of oil from complex aqueous phase/oil mixtures, where the aqueous phases are deionized water (A,B), acidic water, pH,1.0) (C,D), alkaline water, pH, 12.0) (E,F), artificial sea water (G,H) and river (Brahmaputra, Assam, India) water (I,J).

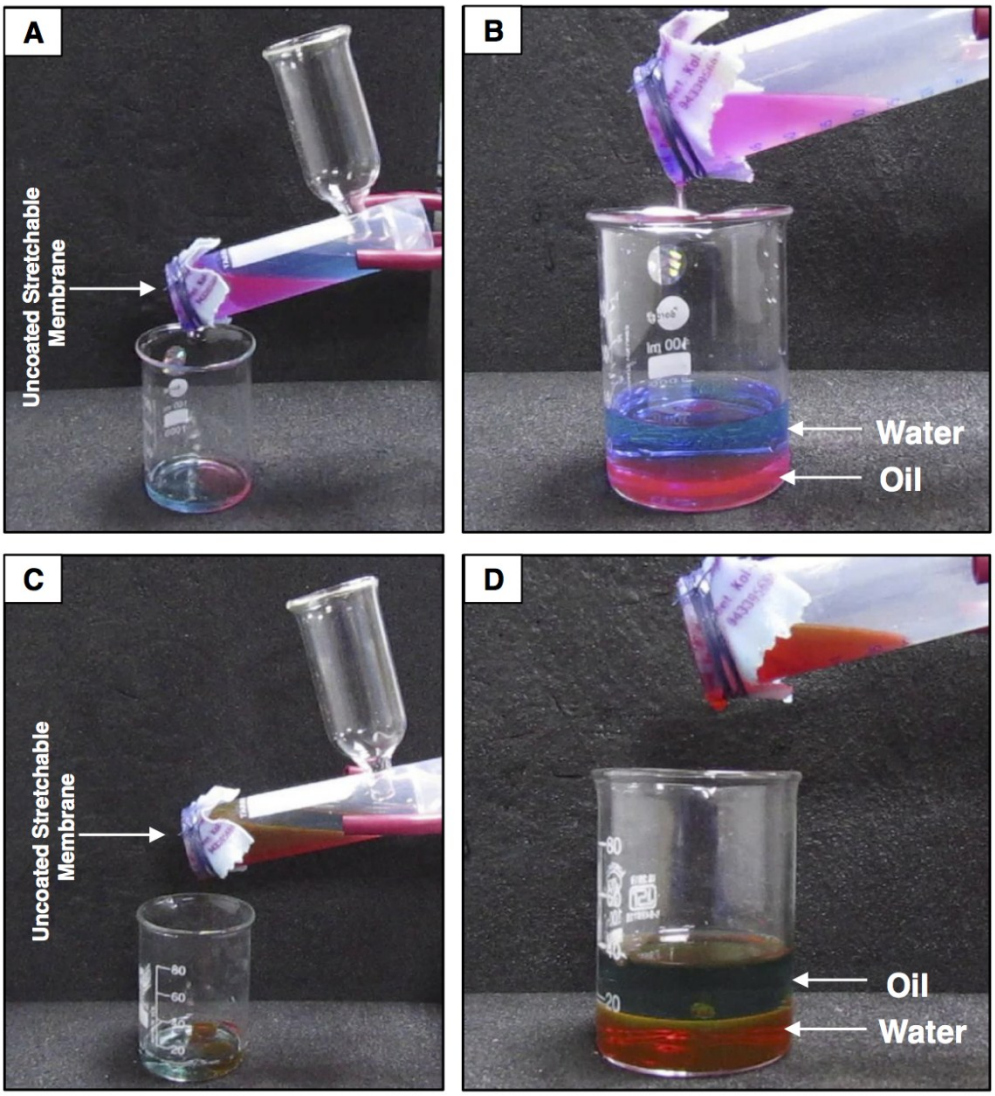


**Figure S13**. (A-D) Digital images illustrating the separation performance of both heavier, DCM) (A, B) and lighter (kerosene) (C, D) oils from corresponding oil/water mixtures using uncoated fibrous PU membrane, where both oil and water layer is passing through the fabric on pouring the oil /water mixture in the prototype.

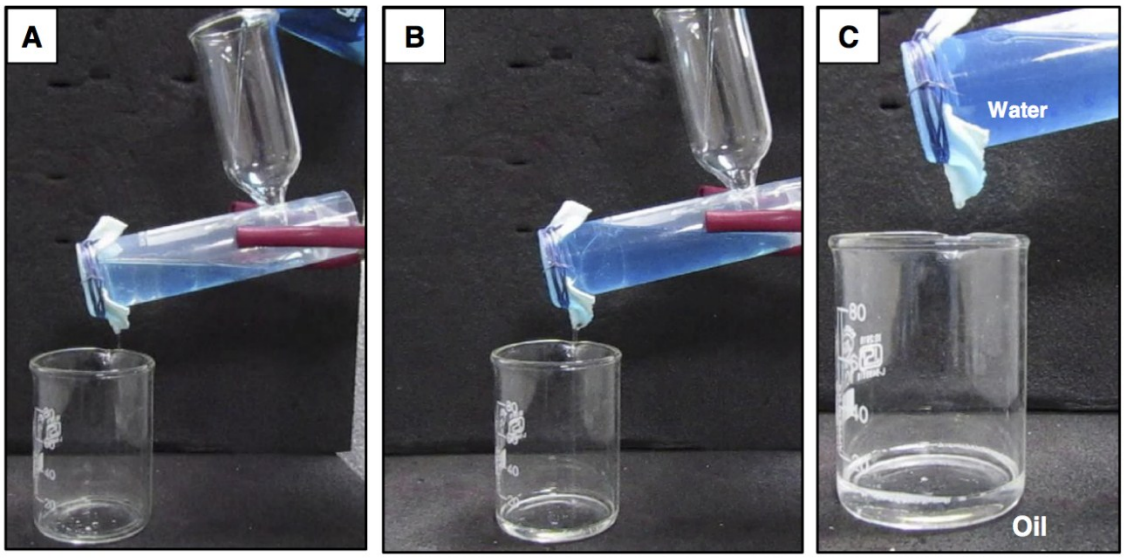


**Figure S14**. A-C) Digital images are depicting the separation of viscous oil (silicon oil) from oil/water mixture, blue color water (due to methylene blue dye) aids visual inspection.

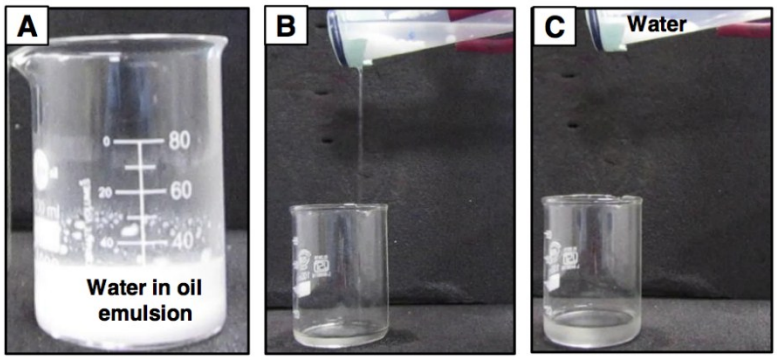


**Figure S15**. A) Digital image of water in oil emulsion. B-C) Illustrating the separation and collection of oil from water in oil emulsion.